Invited Lectures

AMAS Workshop on Nondestructive Testing of Materials
NTM'03 - (pp.13–34) - Warsaw, May 19-21, 2003.

Ultrasonic analysis of texture and characterization of materials properties and behaviour influenced by texture

E. SCHNEIDER and R. HERZER

Fraunhofer Institute for Non Destructive Testing (IZFP)
Saarbrücken, Germany
Schneider@fhg.izfp.de

1. Introduction

Texture causes direction dependencies of the elastic properties. Hence, the ultrasonic wave velocities become direction dependent. The velocities of ultrasonic waves propagating through a textured material with orthorhombic symmetry can be described in terms of the elastic moduli and the 4^{th} order expansion coefficients of the orientation distribution function (ODF). It was in the years following 1982 when the elastic anisotropy caused by texture gained the interest of those researchers working in the field of ultrasonic stress analysis. The objective of the investigations was the separation of the influence of texture on the ultrasonic quantities form those of the stress state. The IZFP activities started in 1984 when the equations published by Sayers [1] are used to study the influence of texture on the temperature dependence of ultrasonic velocities [2]. First results showing the correlation between 4^{th} order expansion coefficients, evaluated using ultrasonic velocity data, and the drawability parameters, characterizing the direction dependence of the plastic deformation of rolled sheets, are published in 1984 [3]. Meanwhile different ultrasonic systems have been developed and introduced into industrial applications.

2. Fundamentals

2.1. Influence of texture on ultrasonic velocities

Most structural materials are polycrystalline aggregates and their exposure to plastic deformation and/or heat treatment during manufacturing

leads to the alignment of the single crystals relative to the forming geometry or the temperature gradient. This development of preferred orientation or texture is the main reason for the anisotropic behaviour of these materials. Electric, magnetic, elastic and plastic properties become direction dependent. This is desirable, for example, for transformer sheets in order to minimize the loss of energy during the magnetic hysteresis. Moreover, a certain texture is also needed in order to optimize the plastic deformation of rolled sheets during the deep drawing of e.g. automotive body parts or food and beverage cans. In other cases, especially designed thermal and/or mechanical treatments are applied to yield components with isotropic properties. Industrial practice for characterizing texture is the measurement of X-ray pole figures from which the expansion coefficients of the orientation distribution function (ODF) are evaluated [4, 5].

The elastic anisotropy caused by texture influences the ultrasonic velocities and is, in addition to the strain or stress state, another reason for the direction dependencies of the wave velocities. Both influences, the texture and the stress superimpose each other. In order to characterize texture the influence of the stress states on the velocities has to be separated or discriminated.

In cubic materials (steels, aluminium-alloys) an orthotropic texture develops, for instance, during rolling. The texture is characterized by three orthogonal mirror planes. Because of the cubic crystal symmetry on the one hand, and the orthotropic texture symmetry on the other hand, in a first approximation only the three fourth-order expansion coefficients C_4^{11}, C_4^{12} and C_4^{13} need to be considered for texture description. The velocities of ultrasonic shear and longitudinal waves, propagating through a stress free cubic material with orthotropic texture are [6]:

$$\rho v_{\mathrm{RR}}^2 = C_{11} - C\left[\frac{2}{5} - \frac{1}{70}\sqrt{\frac{7}{3}}\left(C_4^{11} - \frac{2}{3}\sqrt{5}C_4^{12} + \frac{1}{3}\sqrt{35}C_4^{13}\right)\right], \tag{2.1}$$

$$\rho v_{\mathrm{WW}}^2 = C_{11} - C\left[\frac{2}{5} - \frac{1}{70}\sqrt{\frac{7}{3}}\left(C_4^{11} + \frac{2}{3}\sqrt{5}C_4^{12} + \frac{1}{3}\sqrt{35}C_4^{13}\right)\right], \tag{2.2}$$

$$\rho v_{\mathrm{NN}}^2 = C_{11} - C\left(\frac{2}{5} - \frac{1}{70}\sqrt{\frac{7}{3}}\frac{8}{3}C_4^{11}\right), \tag{2.3}$$

$$\rho v_{\mathrm{RW}}^2 = C_{44} + C\left[\frac{1}{5} + \frac{1}{70}\sqrt{\frac{7}{3}}\left(\frac{1}{3}C_4^{11} - \frac{1}{3}\sqrt{35}C_4^{13}\right)\right] = \rho v_{\mathrm{WR}}^2, \tag{2.4}$$

$$\rho v_{\mathrm{WN}}^2 = C_{44} + C\left[\frac{1}{5} - \frac{1}{70}\sqrt{\frac{7}{3}}\left(\frac{4}{3}C_4^{11} + \frac{2}{3}\sqrt{5}C_4^{12}\right)\right] = \rho v_{\mathrm{NW}}^2, \tag{2.5}$$

$$\rho v_{\mathrm{NR}}^2 = C_{44} + C\left[\frac{1}{5} - \frac{1}{70}\sqrt{\frac{7}{3}}\left(\frac{4}{3}C_4^{11} - \frac{2}{3}\sqrt{5}C_4^{12}\right)\right] = \rho v_{\mathrm{RN}}^2 \tag{2.6}$$

The first subscript of the velocity v indicates the propagation direction, while the second one indicates the polarization direction of the ultrasonic wave. Since the rolling texture is orthotropic and frequently found in half products, this type of texture is chosen to describe the texture influence on ultrasonic velocities. R, W and N represent the rolling, transverse (width) and normal directions, respectively. $C = C_{11} - C_{12} - 2C_{44}$ is the anisotropy factor, a measure of the elastic anisotropy of a single crystal. C_{11}, C_{14}, C_{44} are the single crystal elastic constants. C_4^{11}, C_4^{12} and C_4^{13} are the expansion coefficients according to the Bunge notation. These expansion coefficients carry the texture information. The Roe notation is also often used, so that the following relationships can be helpful:

$$W_{400} = C_4^{11}\frac{\sqrt{2}\sqrt{\frac{7}{3}}}{48\pi^2}, \tag{2.7}$$

$$W_{420} = C_4^{12}\frac{\sqrt{\frac{7}{3}}}{48\pi^2}, \tag{2.8}$$

$$W_{440} = C_4^{13}\frac{\sqrt{\frac{7}{3}}}{48\pi^2}. \tag{2.9}$$

As can be seen from Eqs. (2.4), (2.5) and (2.6), the influence of texture on the shear wave velocities remains unchanged if the directions of propagation and vibration are interchanged. The velocity of the longitudinal wave propagating along the normal direction depends only on one expansion coefficient (Eq. (2.3)). It follows from Eqs. (2.5) and (2.6) that combined use of shear wave velocities yield also relationships with one expansion coefficient only:

$$\rho(v_{\mathrm{NR}}^2 + v_{\mathrm{NW}}^2) = 2C_{44} + 2C\left(\frac{1}{5} - \frac{1}{70}\sqrt{\frac{7}{3}}\frac{4}{3}C_4^{11}\right), \tag{2.10}$$

$$\rho(v_{\mathrm{NR}}^2 - v_{\mathrm{NW}}^2) = 2C\frac{1}{70}\sqrt{\frac{7}{3}}\frac{2}{3}\sqrt{5}C_4^{12}, \tag{2.11}$$

and from Eqs. (2.3) and (2.10) the following relationship, which is independent of texture:

$$\rho(v_{\mathrm{NN}}^2 + v_{\mathrm{NR}}^2 + v_{\mathrm{NW}}^2) = C_{11} + 2C_{44}. \tag{2.12}$$

Out of the numerous possibilities of determining the expansion coefficients from Eqs. (2.1)-(2.6) those which fit best the requirement of low error propagation are [3]:

$$C_4^{11} = \frac{210}{8C}\sqrt{\frac{3}{7}}\left(2\mu - (C_{11} + 2C_{44})\,\frac{v_{\mathrm{NR}}^2 + v_{\mathrm{NW}}^2}{v_{\mathrm{NR}}^2 + v_{\mathrm{NW}}^2 + v_{\mathrm{NN}}^2}\right), \tag{2.13}$$

$$C_4^{12} = \frac{210}{4\sqrt{5}C}\sqrt{\frac{3}{7}}\left((C_{11} + 2C_{44})\,\frac{v_{\mathrm{NR}}^2 - v_{\mathrm{NW}}^2}{v_{\mathrm{NR}}^2 + v_{\mathrm{NW}}^2 + v_{\mathrm{NN}}^2}\right), \tag{2.14}$$

$$C_4^{13} = \frac{210}{8\sqrt{35}C}\sqrt{\frac{3}{7}}\left(6\mu - \lambda + (C_{11} + 2C_{44})\,\frac{v_{\mathrm{NN}}^2 - 8v_{RW}^2}{v_{\mathrm{NR}}^2 + v_{\mathrm{NW}}^2 + v_{\mathrm{NN}}^2}\right), \tag{2.15}$$

$$C_4^{11} = \frac{210}{2C}\sqrt{\frac{3}{7}}\left(\rho(v_{\mathrm{SH0}}^2(0^\circ) + v_{\mathrm{SH0}}^2(45^\circ)) - 2\mu\right), \tag{2.16}$$

$$C_4^{13} = \frac{210\mu}{32\sqrt{35}C}\sqrt{\frac{3}{7}}\left(1 - 2\cos^2\theta\right)^{-2} \cdot \left(1 - \sqrt{1 - 16\frac{(1 - 2\cos^2\theta)^2}{\cos^2\theta\sin^2\theta}\,\frac{v_{SH0(\theta)} - v_{SH0(0^\circ)}}{v_{SH0(0^\circ)}}}\right). \tag{2.17}$$

Here v_{SH0} is the velocity of a shear wave (shear horizontal) propagating through the rolled product along directions with a given angle to the rolling direction.

Of course, the elastic anisotropy of a single crystal has the strongest influence on the direction dependence of the ultrasonic velocities. Table 1 gives the equations for ultrasonic velocities propagating through a material with cubic symmetry.

The (quasi) isotropic polycrystalline material characterizes the other extreme situation. There is no direction dependence of ultrasonic wave velocities. The three fourth-order expansion coefficients C_4^{11}, C_4^{12} and C_4^{13} in Eqs. (2.1)-(2.6) are zero; the ultrasonic velocities are:

$$\rho v_L^2 = C_{11} - 2\frac{C}{5}, \tag{2.18}$$

$$\rho v_T^2 = C_{11} + \frac{C}{5}, \tag{2.19}$$

TABLE 1. Longitudinal and shear wave velocities propagating through a single crystal with cubic symmetry along the principal directions. The subscripts of the shear wave velocities give the direction of wave vibration. The column gives the direction of propagation.

Direction	Longitudinal wave	Shear wave
[100]	$\rho v^2 = C_{11}$	$\rho v^2_{[010]} = C_{44}$ $\rho v^2_{[001]} = C_{44}$
[110]	$\rho v^2 = C_{11} - \frac{1}{2}(C_{11} - C_{12} - 2C_{44})$	$\rho v^2_{[1\bar{1}0]} = C_{44} + \frac{1}{2}(C_{11} - C_{12} - 2C_{44})$ $\rho v^2_{[001]} = C_{44}$
[111]	$\rho v^2 = C_{11} - \frac{2}{3}(C_{11} - C_{12} - 2C_{44})$	$\rho v^2_{[11\bar{1}]} = C_{44} + \frac{1}{3}(C_{11} - C_{12} - 2C_{44})$ $\rho v^2_{[1\bar{1}1]} = C_{44} + \frac{1}{3}(C_{11} - C_{12} - 2C_{44})$

The equations (2.18) and (2.19) describe the longitudinal wave (v_L) and shear wave (v_T) velocities in terms of the density ρ and the single crystal elastic constants according to Voigt notation [7]. The equations most often used in characterization of ultrasonic materials are as follows:

$$\rho v_L^2 = \lambda + 2\mu, \tag{2.20}$$

$$\rho v_T^2 = \mu, \tag{2.21}$$

where λ and μ are the material dependent Lamé constants.

2.2. Determination of the principal axis of texture

The basic equations (2.1)-(2.6), describing the influence of texture on the ultrasonic velocities, presume that the ultrasonic waves propagate and vibrate along principal axes of texture. For the ultrasonic texture analysis on components it is also assumed that the principal axes of residual or load stress coincide with the principal axis of texture. Fortunately, the rolling direction of rolled product as one of the principal texture directions is often known. In other practical cases the determination of the principal axis of texture is the first step to take for the ultrasonic texture characterization.

The use of the ultrasonic birefringence of linearly polarized shear waves is straightforward for that purpose. A linearly polarized shear wave, propagating through the thickness is reflected at the opposite surface of the plate and a backwall echo is received. Multiple thickness propagations yield a backwall echo sequence.

Turning the probe, that is also turning the direction of vibration with respect to the two principal directions of the plane, the backwall echo sequence shown in the upper part of Fig. 1 can only be received if the direction of polarization coincides with a principal axis. In the case of coincidences of both, the direction of polarization and one of the principal directions, the linearly polarized shear wave keeps its linear polarization. The amplitudes decrease due to attenuation effects. In case of no coincidence of both directions, the shear wave vibrates elliptically. The elliptical vibration can be described in terms of the superposition of two wave components, each vibrating parallel to the principal axis. The shape of the ellipse depends on the angle between the incident polarization direction and the principal axis as well as on the difference of the velocities of the wave components.

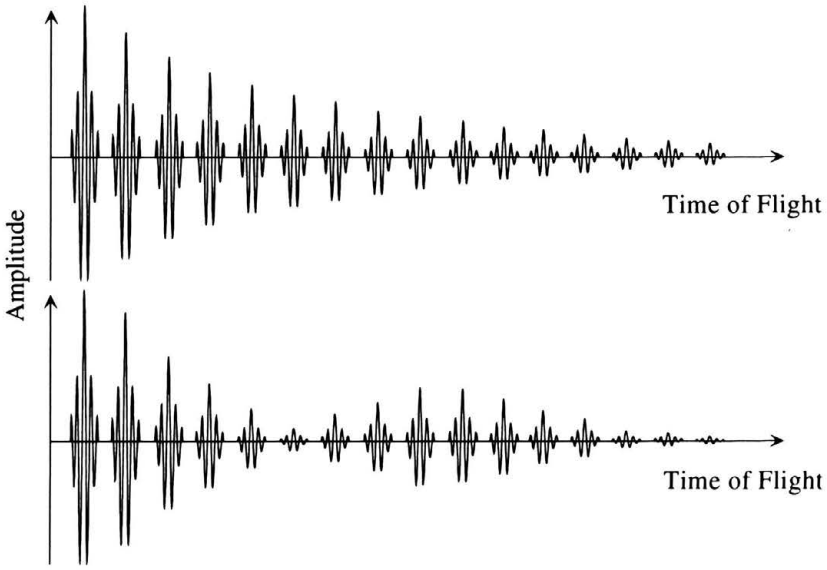

FIGURE 1. Ultrasonic Back Wall Echo Sequence. Vibration direction of incident shear wave parallel (top) and under 45° (bottom) to principal texture axes.

If the angle between the incident vibration direction and the principal axis is 45°, a backwall echo sequence appears as shown in the lower part of Fig. 1. The two wave components of the incident wave have not only the same frequency but approximately about the same amplitudes. The different velocities of the two wave components cause a phase shift between the components which increases with the ultrasonic path. If this phase shift reaches 1/2 ultrasonic wavelength, a destructive interference occurs.

Turning the ultrasonic probe with known polarization direction, the direction is found under which the destructive interference appears. The principal axes are under $\pm 45°$ to a certain polarization direction. By adjusting the vibration direction of the incident wave parallel to each of the principle axes, the extreme values of the ultrasonic velocity or time-of-flight confirm these directions [8].

2.3. Characterization of plastic anisotropy

From the point of view of applications, it is most often not the texture by itself which is of interest, but its consequence, the plastic anisotropy. The plastic anisotropy determines the deep drawability of rolled products. For the characterization of the deep drawing properties the Lankford-parameter, also called r-value, is widely used [9]. This value is determined in a tensile test where the changes of thickness d and width b of a strip is measured after a plastic deformation of at least 20%. The r-value is evaluated according to the relationship

$$r = \frac{\ln(b_0/b_\varepsilon)}{\ln(d_0/d_\varepsilon)}. \tag{2.22}$$

The subscript 0 designates the initial, and the subscript ε the final state of deformation. The quantity q has also found widespread application. It is defined by:

$$q = \frac{r}{r+1}. \tag{2.23}$$

The deep drawability and the effect of earing, respectively, are characterized by the two values r_m and Δr [10]:

$$r_m = \frac{1}{4}\left[r(0°) + 2r(45°) + r(90°)\right], \tag{2.24}$$

$$\Delta r = \frac{1}{2}\left[r(0°) - 2r(45°) + r(90°)\right]. \tag{2.25}$$

They are determined according to Eq. (2.22) using strips cut at 0°, 45° and 90° to the rolling direction.

Investigations using a large number of low-carbon steel sheets confirmed linear correlations between E_m and r_m and ΔE and Δr, respectively [11]. E_m and ΔE are evaluated according to the Eqs. (2.24) and (2.25) as:

$$E_m = \frac{1}{4}\left[E(0°) + 2E(45°) + E(90°)\right], \tag{2.26}$$

$$\Delta E = \frac{1}{2}\left[E(0°) - -2E(45°) + E(90°)\right]. \tag{2.27}$$

The linear correlations between the fourth-order expansion coefficients and the plastic anisotropy parameters r_m and Δr result from empirical relationships between the r-value and the Young's modulus on the one hand and the theoretical relationship between Young's modulus and the fourth-order expansion coefficients on the other hand.

The theoretical relationship between the fourth-order expansion coefficients and the Young's modulus E is described by Bunge [12]. This relationship states that Young's modulus E measured in a certain direction to the rolling direction, described by the angle θ, can be written as

$$E(\theta) = E_r + E_1 C_4^{11} + E_2 C_4^{12} \cos 2\theta + E_3 C_4^{13} \cos 4\theta. \tag{2.28}$$

Here E_r is the average mean value of Young's modulus, and E_1, E_2 and E_3 are constants characterizing the single crystal elastic constants. The direction dependence of the Young's modulus E of textured steel sample was investigated in [13]. Using the single crystal elastic constants and the fourth-order expansion coefficients (calculated from X-ray pole figures) the polycrystalline elastic constants were calculated according to Reuss, Voigt and Hill models.

It follows from the calculation of $E(0°)$, $E(45°)$ and $E(90°)$ according to Eq. (2.28) and from the calculation of E_m and ΔE according to Eqs. (2.26) and (2.27) that there is a linear correlation between C_4^{11} and E_m on the one hand and C_4^{13} and ΔE on the other hand. As mentioned above, there are correlations between E_m and r_m and ΔE and Δr, respectively.

Thus, by determining the expansion coefficients of the fourth-order, ultrasonic techniques offer a possibility to determine parameters which characterize the plastic anisotropy of rolled sheets.

It is often sufficient to measure the direction dependence of the Young-modulus: a large number of established techniques to characterize the drawability behaviour take advantage of Eqs. (2.26) and (2.27). They correlate experimentally evaluated values of E_m and ΔE with r_m and Δr. The techniques differ only in the way of evaluation of the E-modulus.

Since the ultrasonic velocity depends on the elastic properties of the material, the measurement of the direction dependence of the velocity also enables the characterization of the drawability.

As can be seen from Eq. (2.28), the fourth-order expansion coefficient C_4^{12} and the coefficient C_4^{13} are connected with the two fold symmetry ($\cos 2\theta$) and the four fold symmetry ($\cos 4\theta$) of the angle dependence of $E(\theta)$, respectively.

2.4. Characterization of mechanical properties influenced by texture

Ultrasonic velocities are determined by the density and elastic properties of the material. The elastic and elastic/plastic properties of a material or of a component are influenced by numerous structural elements like grains, grain boundaries, second phases, precipitates, pores, dislocations, interstitials, vacancies etc. The same structural elements, as well as the rolling and the heat treatment conditions, determine the development and the degree or strength of the texture.

Hence it is meaningful to investigate the possibility to evaluate the mechanical properties characterized by the yield strength Rp0.2 and the ultimate yield strength Rm by the measurement of the direction dependence of ultrasonic velocities or times-of-flight.

3. Measuring set-ups and sensors

Since the ultrasonic texture analysis is based on the evaluation of the ultrasonic velocities and their direction dependence, the set-ups and sensors are identical with those used for ultrasonic stress analysis, as they are described in [14, 15]. Set-ups to measure the ultrasonic time-of-flight with a relative accuracy better than 0.01% are available on the market. A large variety of sensors are also available. They have to be selected for each case of application, depending on the geometry of the component and on the most suitable combination of the evaluation equations, given before.

The use of electromagnetic transducers (EMATs) is of particularly advantageous since they do not need a coupling medium. By the superposition of magnetic and electric fields, shear waves are generated in the material. The manipulation of EMATs is simplified since they allow a gap between the surface of the component and the sensor. However, the surface of rolled sheets should not be scratched [16, 17, 18].

The sensor shown in the left part of Fig. 2 generates and receives shear horizontal waves (SH-waves). The sensor is designed for in line texture analysis and evaluation of drawability parameters on moved strips. The ultrasonic frequency is 400 kHz, the wavelength is 8 mm, the receiver-receiver distance is 80 mm. The sensor enables measurements with an air gap between the sensor and the surface of the ferritic steel strip of about 2 mm. Similar sensors are also built for the texture analysis on Al rolled products. The sensor shown in the left part of the figure is a EMAT also. It generates and receives a linearly polarized shear wave with a centre frequency of about 2 MHz. The size of the aperture is about 15 mm × 15 mm.

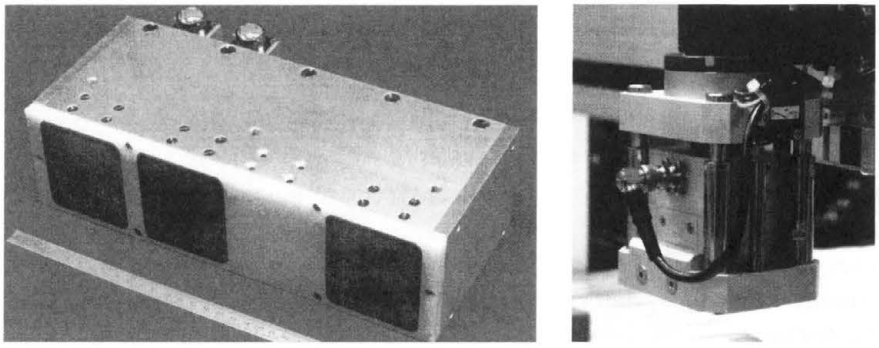

FIGURE 2. Ultrasonic sensor containing three electromagnetic ultrasonic transducers (EMATs) for texture analysis on moved strips (left). There are one transmitting and two receiving EMATs. EMAT sensor for linearly polarized shear wave with normal incidence (right).

An ultrasonic set-up for automated analysis of texture is shown on the left side of Fig. 3. The set-up uses a linearly polarized, normal incident shear wave and measures the ultrasonic time-of-flight as function of the polarization direction with respect to the rolling direction. The relative change of the time-of-flight is a direct measure for the size of the elastic anisotropy caused by texture and the shape of the measured curve gives information on the sharpness of the texture. The right side of the figure shows an ultrasonic set-up for stress and texture analysis. The set-up enables to use both electromagnetic and piezoelectric transducers. It measures the time-of-flight and

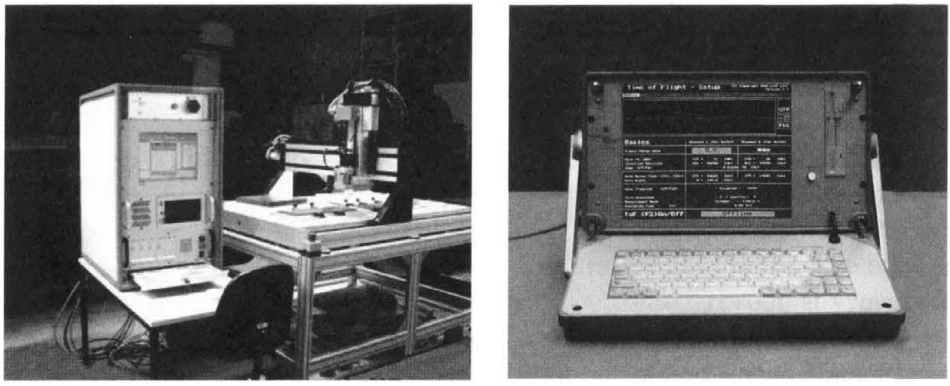

FIGURE 3. Ultrasonic set-up for automated texture analysis at different positions along a rolled part (left) and ultrasonic device for stress and texture analysis (right).

evaluates the state and the property using stored material dependent data and appropriate equations or correlation functions.

4. Results of ultrasonic characterization of texture and properties

4.1. Characterization of texture

The characterization of the texture in terms of the fourth-order expansion coefficients according to Eqs. (2.1)-(2.6) can only be done if the samples shape enables the wave propagation along the principal axes of the texture. Comparisons of the expansion coefficients evaluated using the X-ray pole figures and using sound velocity data show reasonable agreements [6]. It has be taken into consideration that X-ray diffraction analyses a surface near layer of some ten micrometers whereas the ultrasonic waves cover either a surface layer of some millimeters or the whole thickness of the sample. Using ultrasonic microscopy techniques, the analysis of thin surface layers is of course possible, but this technique has not yet been used for texture analysis. The direction dependent values of the E modulus of a textured steel plate are calculated and a good agreement is found with the modulus evaluated using the ultrasonic velocities [13].

However, the use of ultrasonic waves to determine the texture is rather limited since the fourth-order expansion coefficients only can be evaluated using ultrasonics. The X-ray technique enables the evaluation of higher order coefficients as well. Higher-order expansion coefficients are needed to model the plastic deformation.

The advantage of the ultrasonic technique is the fast qualitative characterization of the texture. The relative change of ultrasonic velocities or, in case the ultrasonic path length remains unchanged, the ultrasonic times-of-flight with the change of the propagation or vibration direction with respect to the texture axes is a direct measure for the strength of the texture.

Applying a linearly polarized shear wave propagating through the thickness of a rolled plate enables the characterization of the texture and visualization of the two fold texture symmetry. The left part of Fig. 4 displays the relative change of the time-of-flight versus the direction of polarization. 0° corresponds with the vibration direction parallel to the rolling direction.

The application of SH wave results in the visualization of the fourfold texture symmetry. The SH wave propagates between transmitting and receiving EMAT transducers in the plane of the rolled sheet and vibrates in the direction perpendicular to the propagation direction. If the propagation occurs along the rolling direction, the vibration is along the width direction

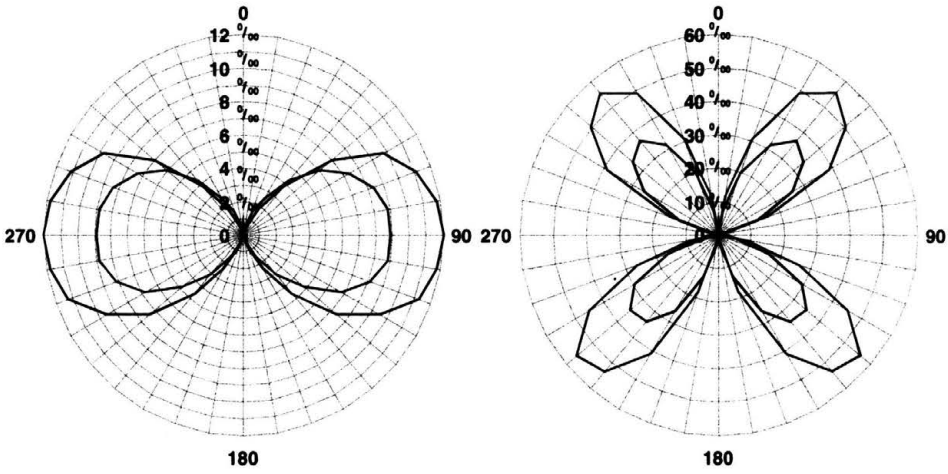

FIGURE 4. Relative change of the time-of-flight of shear wave propagating through the thickness of rolled plates versus the direction of polarization. 0° corresponds to the vibration direction parallel to the rolling direction (left). Relative change of the time-of-flight of SH wave versus the direction of propagation. 0° means that the propagation is along the rolling direction (right). The figure shows results for two rolled plates with differently developed texture.

and vice versa. As can be seen from Eqs. (2.4)-(2.6) the influence of rolling texture on the shear wave velocity remains unchanged if the directions of polarization and vibration are interchanged.

The right part of Fig. 4 shows the relative change of the time-of-flight of SH wave versus the direction of propagation. 0° means that the propagation direction is along the rolling direction. The figure shows two results found using two rolled plates with differently developed texture.

As can be seen from Eq. (2.28) $E(\theta) = E_r + E_1 C_4^{11} + E_2 C_4^{12} \cos 2\theta + E_3 C_4^{13} \cos 4\theta$, the twofold and fourfold symmetry are related to the expansion coefficients C_4^{12} and C_4^{13}, respectively. Hence, the application of SH wave gives information on the expansion coefficient C_4^{13} and Δr and the application of a shear wave gives information on C_4^{12} (see Section 4.2).

In some cases of application the following procedure is helpful. Using the single crystal elastic constants the velocities of longitudinal and shear waves propagating along the particular direction can be evaluated. The left part of Fig. 5 shows the velocities triangle for Fe and Al single crystal. The higher degree of isotropy of the Al single crystal compared with the Fe data is clearly seen. In some materials and alloys the texture changes with slight changes of the heat treatment conditions. As a result, the point given by the longitudinal and shear wave velocity is closer to the direction pole [111] if

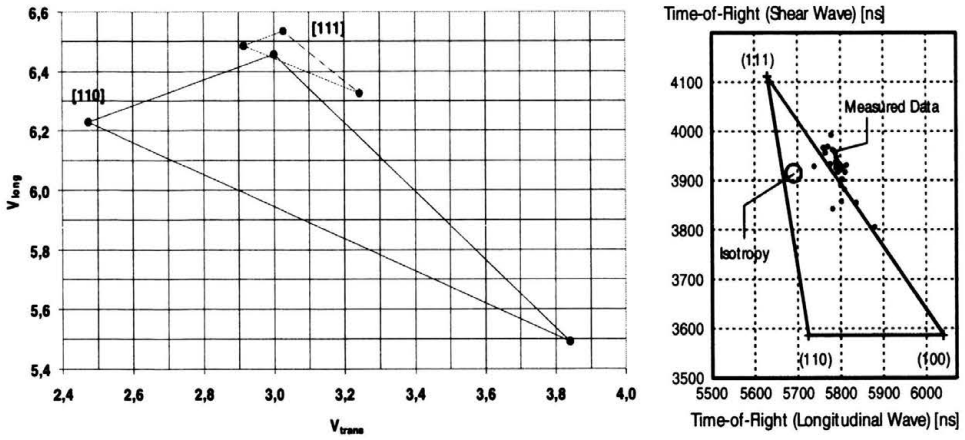

FIGURE 5. Orientation of the velocities of longitudinal and shear wave propagating along the given direction of a Fe and Al single crystal (left). Results of an investigation using rolled Ta plates (right).

most of grains of the polycrystalline material have their [111] direction along the propagation direction of the waves.

The right part of the figure shows results of the characterization of the texture of Ta plates. In that particular application, the thickness of the plates was identical, hence the measurement of the ultrasonic time-of-flight was sufficient. The waves propagate through the thickness. The position of the measured data correlates with the direction dependence of the plastic deformation of rolled Ta plates.

4.2. Evaluation of drawability parameters

The non destructive characterization of the drawability of rolled products is of industrial interest. In order to confirm the correlations, as described in Section 2.3, numerous experimental investigations have been made. As shown in Fig. 6 the estimated correlations are experimentally confirmed. In Fig. 7 the result of the on-line-evaluation of the drawability parameters using ultrasonic technique are to be seen. The strip moved with the velocity of about 120 m/min [19].

As can be concluded from Fig. 4 and from the fundamental Eqs. (2.11) and (2.26)-(2.28), the relative change of the velocity or time-of-flight of SH wave propagating along the rolling direction and under 45° to it carries the texture information. Hence, it is sufficient to use this ultrasonic quantity in order to evaluate the drawability parameter Δr and experimentally established correlations as the one shown in Fig. 8.

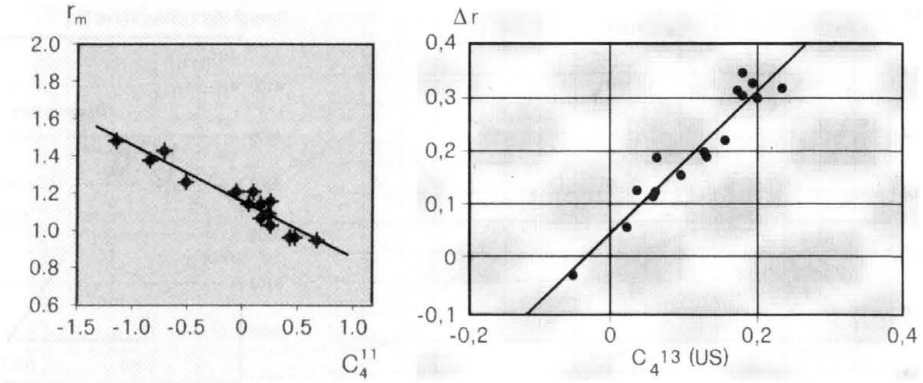

FIGURE 6. Correlation between the fourth-order expansion coefficients C_4^{11} and C_4^{13}, evaluated using ultrasonic velocity data and the drawability parameters of rolled steel sheets [6].

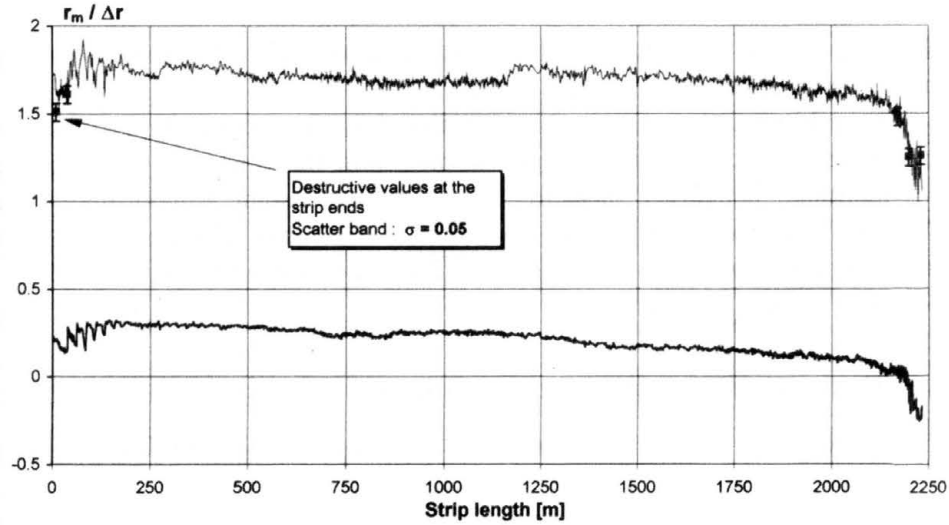

FIGURE 7. Drawability parameters evaluated on-line on the moving strip using ultrasonic technique and the results of the established destructive technique (points) [19].

Figure 9 illustrates on its left side the relative change of the SH wave time-of-flight versus the direction of propagation in rolled Al sheets. That particular result shows no significant difference between the texture influence measured in the middle of the width of the rolled strip or close to its edge. In the right side of the figure, the good correlation between the ultra-

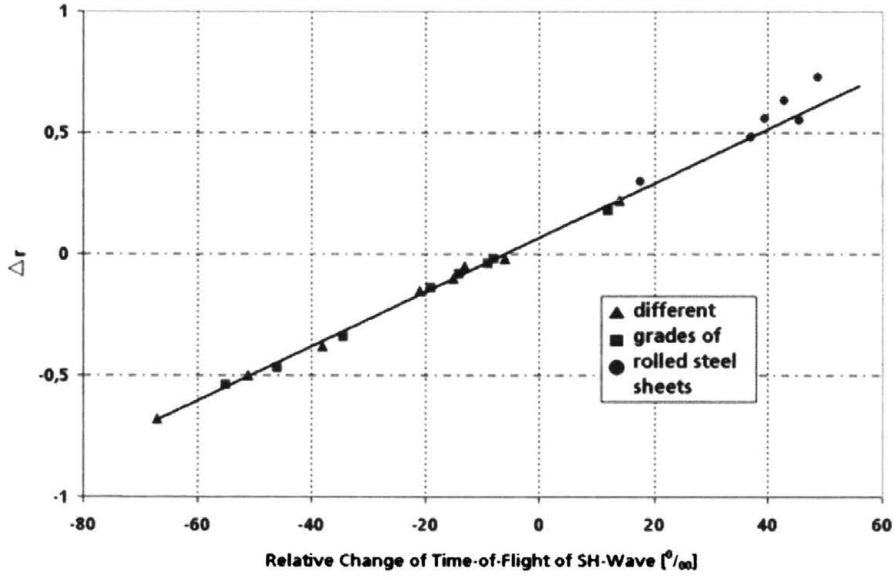

FIGURE 8. Correlation between the relative change of time-of-flight of SH wave propagating along the rolling direction and under 45° to it and the drawability parameter Δr of different grades of steel sheets.

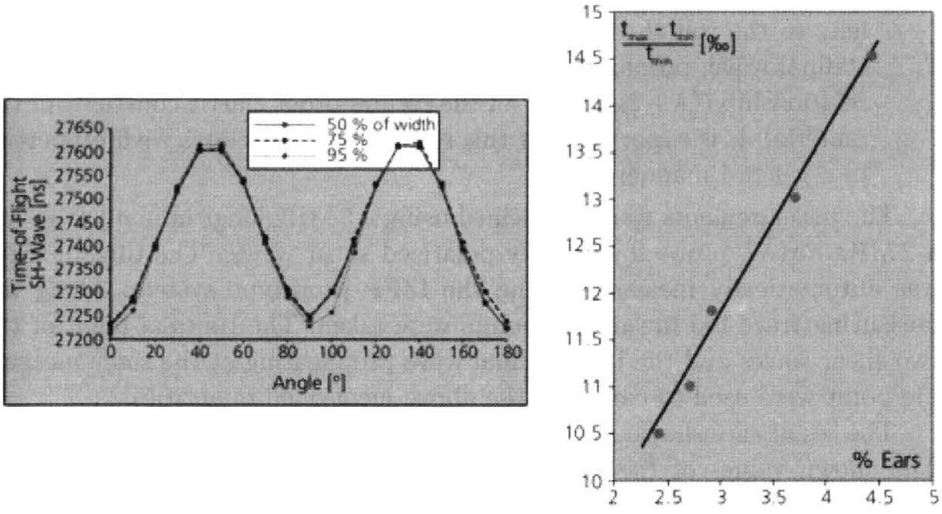

FIGURE 9. Relative change of the SH wave time-of-flight versus the direction of propagation in rolled Al sheets (left) and the correlation between the relative change of time of flight with the earing parameter (right).

sonic quantity and the earing parameter demonstrates the applicability of the technique for rolled Al products [20].

4.3. Evaluation of yield strength

Influence of microstructural elements on the elastic behaviour and hence on the ultrasonic velocities is small. In order to optimize the sensitivity and the measuring accuracy, it is avoided to evaluate the absolute values of the velocities of ultrasonic waves. The ultrasonic time-of-flight can be measured with an accuracy better than 1 in 10^4; the measurement of the ultrasonic path length or the components thickness with a similar accuracy is at least very time consuming and often difficult to perform on components. In order to get quantities, independent of the thickness of the component under test, the following two techniques are found to be very suitable:

1. The evaluation of the relative difference of the time-of-flight $(t_R - t_W)/t_W$ [%] of two shear waves propagating through the thickness with polarizations parallel (R) and perpendicular (W) to the rolling direction of the material. The relative difference is a measure of the elastic anisotropy caused by texture. It is expected that this quantity correlates with the elastic and elastic/plastic properties of materials and components with a strongly developed texture.
2. The evaluation of the time-of-flight of the shear wave polarized parallelly to the rolling direction, related to the time-of-flight of the longitudinal wave, propagating along the thickness (t_R/t_{Long}) results in the relationship $((\lambda+2\mu)/\mu)^{1/2}$ of the second-order elastic constants of the material. It is expected that this relationship correlates with properties in a general manner.

The measurements were performed using a 5 MHz longitudinal probe and a 2 MHz EMAT probe for linearly polarized shear waves. The time-of-flight was automatically measured using the IZFP prototype system. Along the measuring trace ten measuring points were taken. The times-of-flight of the two shear waves and the longitudinal wave propagating at the same measuring point were used to calculate the above mentioned quantities.

The results are shown in Figs. 10-14 together with the error bars if known. The shown values of the ultrasonic quantities are the mean values of ten measurements at different positions of the particular steel sample. Up to now, there are only useful correlations found for materials with a strongly developed texture.

The elastic anisotropy, characterized by the relative difference of time-of-flight $(t_R - t_W)/t_W$ [%] is found to be very significant in the thermomechan-

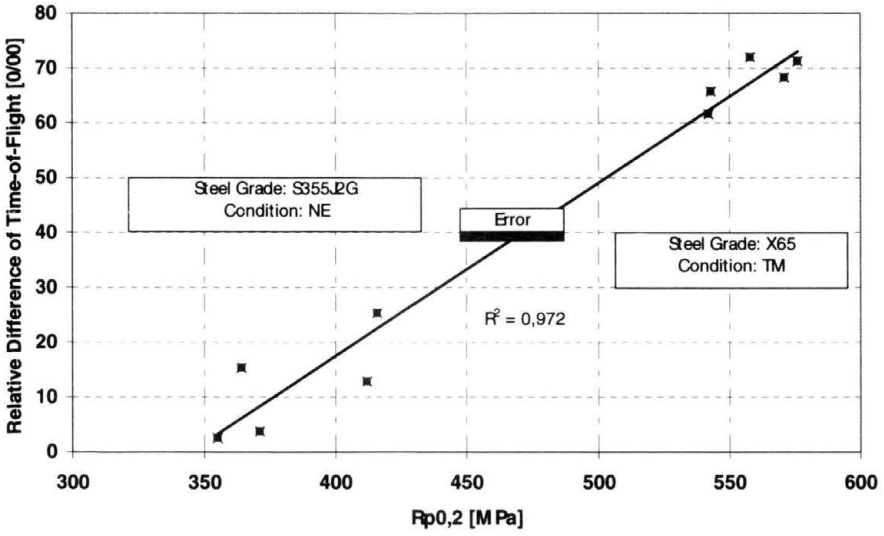

FIGURE 10. Correlation of the relative difference of the time-of-flight $(t_R - t_W)/t_W$ [%] of two shear waves propagating through the thickness with polarizations parallel (R) and perpendicular (W) to the rolling direction with the Rp0.2 value of samples of two steel grades.

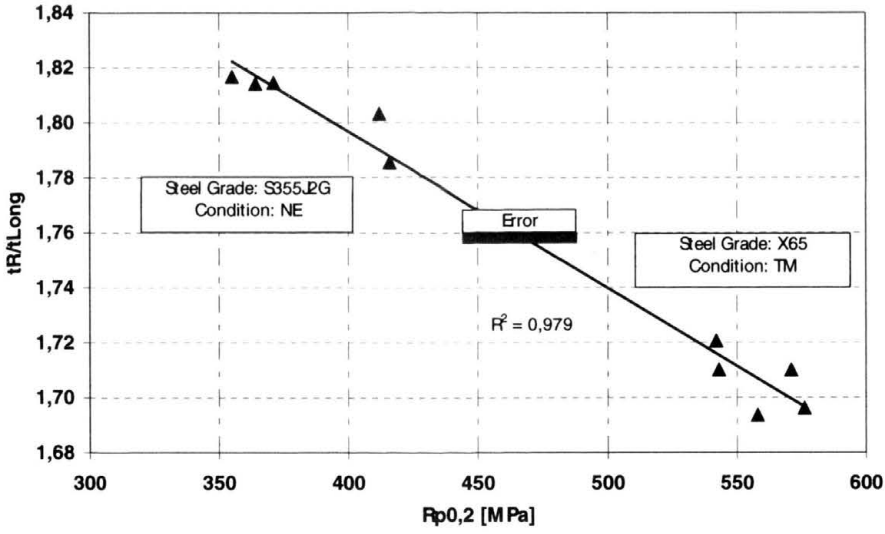

FIGURE 11. Correlation of the time-of-flight of the shear wave polarized parallel to rolling direction (t_R) related to the time-of-flight of the longitudinal wave (t_{Long}), with the Rp0.2 value of samples of two steel grades.

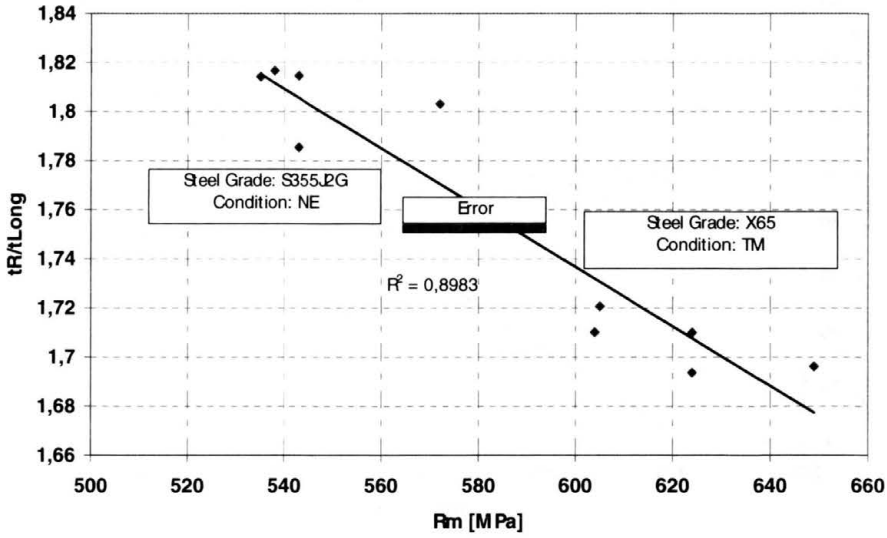

FIGURE 12. Correlation of the time-of-flight of the shear wave polarized parallel to rolling direction (t_{R}) related to the time-of-flight of the longitudinal wave (t_{Long}), with the Rm value of samples of two steel grades.

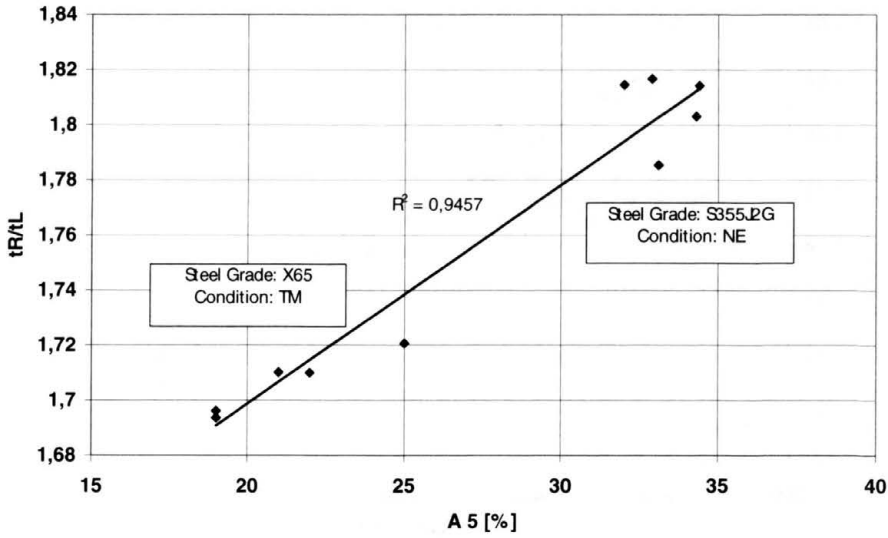

FIGURE 13. Correlation of the time-of-flight of the shear wave polarized parallel to rolling direction (t_{R}) related to the time-of-flight of the longitudinal wave (t_{Long}), with the A5 value of samples of two steel grades.

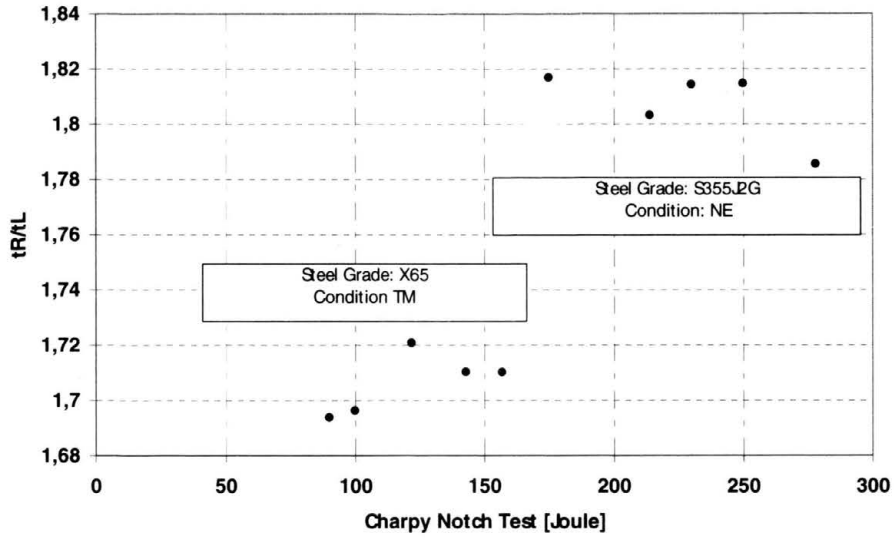

FIGURE 14. Correlation of the time-of-flight of the shear wave polarized parallel to rolling direction (t_R) related to the time-of-flight of the longitudinal wave (t_{Long}), with the result of the Charpy Notch test of samples of two steel grades.

ically rolled (TM) plates and to a lower degree in the rolled and annealed (NE) plates, also.

As expected, there are correlations between the elastic anisotropy, characterized by ultrasonic quantities, and the technological data of the tested steel grades.

The values of the Charpy Notch Test of the samples of both steel grades cannot be approximated by one correlation line (Fig. 17); it seems to be possible to correlate the data for each individual steel grade in an acceptable way.

The accuracy of the relative difference of the time-of-flight $(t_R - t_W)/t_W$ is better than $\pm 0.02\%$, the accuracy of the values t_R/t_{Long} is better than ± 0.005. The achievable accuracy of the Rp0.2 and Rm values using the correlations as found is mainly determined by the accuracy of the Rp0.2 and Rm values, evaluated by established tensile test experiments.

5. Summary

The state of IZFP developments is presented. A short review of the ultrasonic background is given and the sensors and the measuring set-ups are shown. The results of different cases of laboratory and in field applications are described.

Texture causes direction dependencies of the elastic properties. Hence, the ultrasonic wave velocities become direction dependent. The velocities of ultrasonic waves propagating a textured material with the orthorhombic symmetry can be described in terms of the elastic moduli and the fourth-order expansion coefficients of the orientation distribution function (ODF).

Measuring the ultrasonic velocities as a function of the ultrasonic propagation and vibration directions with respect to the texture axes, the fourth-order expansion coefficients are evaluated.

Applying a linearly polarized shear wave, the principal symmetry axes of the texture are determined and by measuring the ultrasonic time-of-flight as function of the polarization direction, the two axial symmetry of the texture is characterized. Measurements of the time of flight of SH wave as a function of the propagation direction enable the characterization of the four axial symmetry of the texture.

The texture in steel sheets and plates, in rolled Al products and in Ta samples is determined by the mentioned measurements.

Using correlations between the elastic anisotropy, evaluated in terms of the direction dependent change of the ultrasonic velocities or times-of-flight, the drawability parameters of cold rolled ferritic and austenitic steel strips are evaluated as well as the earing parameters of hot rolled aluminium sheets.

Fast and easy to apply ultrasonic measurements are seen as a substantial support to efforts of optimization of rolling process and heat treatment and to control the recrystallization, the development of the texture and the drawability.

Since the elastic and anelastic properties of a single crystal are direction dependent, and since the texture characterizes the non statistical orientation of the single crystals in a polycrystalline metal, it is possible to find correlations between material properties like, e.g. the yield strength and the texture dependent ultrasonic quantities.

References

1. C.M. SAYERS, Ultrasonic velocities in polycrystalline aggregates; *J. Phys. D.; Appl. Phys.*, Vol.15 (1982), pp.2157-2167.

2. E. SCHNEIDER, S.L. CHU, K. SALAMA, Influence of texture on the temperature dependence of ultrasonic velocities, *IEEE 1984 Ultrasonic Symposium* (1984), pp.944-949.

3. M. SPIES; E. SCHNEIDER, Zerstörungsfreie Analyse von Texturen in Walzprodukten mit Ultraschallverfahren, *Deutsche Gesellschaft für Zerstörungsfreie Prüfverfahren e.V. DACH Jahrestagung, Berichtsband 10, Teil 1* (1987) pp.122-128.

4. H.J. BUNGE, Zur Darstellung allgemeiner Texturen, *Z. Metallkunde*, Vol.56 (1965), pp.872-874.

5. R.J. ROE, Description of crystallite orientation in polycrystalline materials, general solution to pole figure inversion, *J. Appl. Phys.*, Vol.36 (1965), pp.2024-2031.

6. M. SPIES, E. SCHNEIDER, Nondestructive analysis of textures in rolled sheets by ultrasonic techniques, *Textures and Microstructures* (1990), No.12, pp.219-231.

7. W. VOIGT, *Lehrbuch der Kristallphysik*, B.G. Teubner Verlag, Leipzig.

8. E. SCHNEIDER, Ultrasonic birefringence effect – its application for materials characterizations, *Optics and Lasers in Engineering*, Vol.22 (1995), pp.305-323.

9. W.T. LANKFORD, S.C. SNYDER, J.A. BAUSCHER, *Trans. ASM*, Vol.42 (1950), p.1197.

10. C.M. VLAD, Verfahren zur Ermittlung der Anisotropie-Kennzahlen für die Beurteilung des Tiefziehverhaltens kohlenstoffarmer Feinbleche, *Materialprüfung* Vol.14 (1970), pp.179-182.

11. C.A. STICKELS, P.R. MOULD, The use of Young's modulus for predicting the plastic strain ratio of low-carbon steel sheets, *Met. Trans.*, Vol.1 (1970), pp.1303-1311.

12. H.J. BUNGE, Über die elastischen Konstanten kubischer Materialien mit beliebiger Textur, *Kristall & Technik*, Vol.3 (1968), pp.431-438.
H.J. BUNGE, Texture Analysis in Materials Science; London: Butterworth Publ. London (1982).
H.J. BUNGE, Mean values of physical properties, in: H.J. Bunge, C. Esling (Eds.), *Quantitative Texture Analysis*, DGM Oberursel (1982), pp.383-405.

13. P. SPALTHOFF, W. WUNNIKE, C. NAUER-GERHARD, H.J. BUNGE, E. SCHNEIDER, Determination of the elastic tensor of a textured low-carbon steel; *Textures and Microstructures*, Vol.21 (1993), pp.3-16.

14. E. SCHNEIDER, Nondestructive evaluation of stress states in components using ultrasonic and electromagnetic techniques, in: J. Deputat, Z. Ranachowski (Eds), *Conference Proceedings 1, Nondestructive Testing of Materials and Structures, AMAS Course – NMT'02*, Institute of Fundamental Technological Research, Polish Academy of Science (2002), pp.61-80.

15. E. SCHNEIDER, *Untersuchungen der materialspezifischen Einflüsse und verfahrenstechnische Entwicklungen der Ultraschallverfahren zur Spannungsanalyse an Bauteilen*, D 82 (Diss. RWTH Aachen), Fraunhofer IRB Verlag Stuttgart 2000.

16. G. HÜBSCHEN, *Senkrecht zur Einfallebene polarisierte Ultraschalltransversalwellen, Elektromagnetische Wandlung, Ausbreitung und Anwendungspotential in der zerstörungsfreien Werkstoffprüfung*, Dissertation, IZFP, Universität des Saarlandes (1986).

17. P. HÖLLER, H.J. SALZBURGER, Ultrasonic testing by electromagnetic transducers – state of technology and applications in industry, in: *International Conference on Monitoring and Predictive Maintenance of Plants and Structures Proceedings* (1992), pp.50-57.

18. G. ALERS, G. HÜBSCHEN, B. MAXFIELD, W. REPPLINGER, H.J. SALZBURGER, R.B. THOMPSON, A. WILBRAND, Electromagnetic acoustic transducers, *ASNT Nondestructive Testing Handbook*, Second Edition, P. McIntire (Ed.), Vol.7 (1991), pp.326-340.

19. M. BORSUTZKI, J. KROOS, W. REIMCHE, E. SCHNEIDER, Magnetische und Akustische Verfahren zur Materialcharakterisierung von Stahlblechen, *Stahl und Eisen*, Vol.120 (2000), No.12, pp.115-121.

20. E. SCHNEIDER, L. OESTERLEIN, Ultrasonic characterization of texture in aluminium rolled products, in: A.L. Bartos, R.E. Green Jr., C.O. Ruud (Eds.), *Nondestructive Characterization of Materials VII*, Transtec Publications Ltd, Zürich, Part 1 (1996), pp.405-410.